ISSN 1063-7842, Technical Physics, 2013, Vol. 58, No. 5, pp. 735–743. © Pleiades Publishing, Ltd., 2013.
Original Russian Text © Yu. Kudriavtsev, R. Asomoza, M. Mansurova, L.A. Perez, V.M. Korol', 2013, published in Zhurnal Tekhnicheskoi Fiziki, 2013, Vol. 83, No. 5, pp. 115–124.

PHYSICS
OF NANOSTRUCTURES

Sputtering of the Target Surface by Cs^+ Ions: Steady-State Concentration of Implanted Cesium and Emission of CsM^+ Cluster Ions

Yu. Kudriavtsev[a] *, R. Asomoza[a], M. Mansurova[b], L. A. Perez[b], and V. M. Korol'[c]

[a] *Department of Electrical Engineering-SEES, CINVESTAV-IPN, Mexico City, 07360 Mexico*
[b] *Institute of Physics, National Autonomous University of Mexico, A. P. 20-364, Mexico City, 01000 Mexico*
[c] *Research Institute of Physics, Southern Federal University, pr. Stachki 194, Rostov-on-Don, 344090 Russia*
**e-mail: yuriyk@cinvestav.mx*

Received May 28, 2012

Abstract—Experimental data for the variation of the work function on the Si and GaAs semiconductor surfaces irradiated by cesium ions are presented. The formation mechanism of CsM^+ cluster ions (M is the analyte) is considered. Ionization potentials for some CsM molecules are calculated, and a simple experimental technique to determine the concentration of cesium penetrating into the subsurface region of various materials during cesium ion sputtering is suggested. This technique uses a preimplanted potassium as an "internal standard."

DOI: 10.1134/S1063784213050125

INTRODUCTION

Ion sputtering of the target surface is widely used for layer-by-layer analysis in fabrication of semiconductor devices and provides a basis for secondary ion mass spectrometry (SIMS). Physically, ion irradiation of materials is a complex process that, among other things, modifies the irradiated surface composition: after irradiation, a thin surface layer of the target represents a mixture of target atoms and implanted primary ions [1]. This circumstance is exploited in advanced SIMS: analytes are irradiated by electrically active cesium and oxygen ions. In the former case, ion implantation results in the formation of a thin oxide layer on the surface [2, 3], and its work function rises. As a consequence, the secondary emission of positive ions grows by two to three orders of magnitude. In the latter case, implanted cesium atoms generate surface electrical dipoles the field of which considerably lowers the work function of the surface. Under these conditions, the secondary emission of negative ions increases by two to three orders of magnitude [4, 5]. The above effects stem from the exponential dependence of the secondary emission of positive and negative ions on the work function of the emitting surface [3],

$$P^{+} \propto \exp[-(I_p - \Phi^*)/\varepsilon_p], \quad (1a)$$

$$P^{-} \propto \exp[-(\Phi^* - A_e)/\varepsilon_n]. \quad (1b)$$

Here, Φ^* is the work function of the target being irradiated by ions; I_p and A_e are, respectively, the ionization potential and electron affinity of an emitted ion; and ε_i is a factor characterizing ion sputtering conditions (in some models of ion generation, this factor is assumed as the instantaneous temperature in a collision cascade [6]).

Although the described effects are of practical importance, the exact concentration of ions implanted into the subsurface layer of the target during ion etching remains unknown. Experimental data for the irradiated surface composition obtained by different authors using Auger electron spectroscopy, X-ray photoelectron spectroscopy, Rutherford backscattering, etc., are contradictory. For example, when silicon is sputtered by cesium ions (the problem that is the best studied today in this area), published data on the surface concentration of cesium vary from 3.4 to 80.0 at % for a cesium ion beam energy from 1 to 10 keV and an angle of incidence of primary ions from 20° to 60° relative to the normal [7–17]. The generation of secondary ions during sputtering is determined by the target's surface composition, and it is therefore clear that such a spread in experimental data does not allow researchers to study the process of secondary ion emission (SIE) and apply the available models of SIE in quantitative SIMS-based analysis.

In this work, the authors make a critical review of the available experimental data on the composition and work function of the ion irradiated surface, suggest a new model of CsM^+ cluster formation during target sputtering, and describe a simple experimental technique for in situ measuring of the cesium concentration on the irradiated surface during ion sputtering of the target.

EXPERIMENTAL

Experiments were conducted with a CAMECA ims-6f (France) mass spectrometer. Sputtering was accomplished by cesium ions with an energy of 5 keV making an angle of 45° with the normal to the surface. A sharply focused ion beam was swept into a 250 × 250-μm raster pattern. Secondary ions emitted from the central area of the raster about 60 μm in diameter were focused by a set of electrostatic lenses on the entrance to the double-focusing mass analyzer in which their energies and masses were analyzed by a spherical 90° energy analyzer and 90° magnetic sector-field analyzer, respectively. The secondary ion current was detected, according to its value, either with a photoelectric multiplier operating in the pulse count mode or with a Faraday cup.

The variation of the work function of the cesium-ion-irradiated target was studied by the method suggested in [18, 19]. The shift of the energy spectrum of emitted cesium ions was measured as a function of the cesium ion irradiation dose. The energy of secondary ions recorded by the mass spectrometer is their intrinsic emission energy plus an energy due to an accelerating potential applied to the target (+5 kV in our case). The intrinsic energy of the ions is reckoned from the Fermi level of the emitting surface; therefore, a decrease or increase in the work function of the target shifts the energy spectrum, which is recorded relative to the work function of the grounded metallic slit of the energy analyzer. The energy spectra of secondary ions are taken by adding a bias potential (±30 V) to the accelerating voltage with the slit of the energy analyzer closed almost completely. In our experiments, the transmission band of the energy analyzer was estimated at a level of 2 eV and the bias potential scan step was 0.5 eV. In essence, the scan step specified the resolution of experimental energy spectra. To limit the secondary ion angular distribution by ions emitted near the normal to the surface, we used a contrast aperture 40 μm in diameter. The zero energy in the secondary ion energy distribution was determined by linearly extrapolating the low-energy part of the energy spectrum to the *x* axis [18, 19].

Si and GaAs test samples were cut from standard polished wafers. Implantation of Na and K alkali ions was carried out on an implanter installed in the Research Institute of Physics (Southern Federal University, Rostov-on-Don). The ion energy was varied from 45 to 70 keV; the implantation dose, in the range $(1–3) \times 10^{15}$ ions/cm^2.

RESULTS AND DISCUSSION

Our technique for measuring the implanted cesium concentration is based on comparative analysis of Cs_2^+ and $CsAlk^+$ ion emissions (Alk^+ stands for an alkali metal, K or Na, preimplanted into the target). Therefore, it is necessary to consider in detail the mechanism of CsM^+ cluster ion formation during target sputtering by cesium ions before discussion of experimental data.

MODEL OF CSM+ CLUSTER ION FORMATION

In relevant publications, a statistical model of CsM^+ cluster ion formation is being widely discussed. In this model, these ions result from recombination of independently sputtered M atoms and Cs ions over the emitting surface [20, 21],

$$Cs^+ + M^0 \longrightarrow CsM^+. \quad (2)$$

The authors of [20, 21] guess that this model explains the almost complete absence of the matrix effect (i.e., the strong dependence of the SIE on the chemical composition of the surface) when III–V semiconductors are analyzed by means of SIMS [22]. We, however, think that the model is contradictory and fails in explaining a large body of experimental data. Specifically, it cannot explain how two sputtered positive cesium ions may combine into Cs_2^+ clusters (in this model, the SIE coefficient for cesium is taken to be equal to unity). Moreover, many recent experiments with, for example, Si, SiGe, SiC, and SiO targets [23–26] have revealed a tangible matrix effect, while model (2) gives no explanation to the fact that the matrix effect is monitored for one target, but is neglected for others. Regarding the recombination of independently sputtered atoms, it is very difficult to explain the experimental fact that the yield of Cs_2F^+ triatomic clusters is three orders of magnitude higher than that of CsF^+ diatomic clusters [27]. Indeed, according to Gerhard [28], the yield of dimers is expected to be one and a half to two orders of magnitude higher than that of trimers. All this gives grounds for putting forward an alternative model of CsM^+ cluster formation during surface sputtering by cesium ions.

The model suggested in [29] is based on the results of computer simulation by the Monte Carlo method and the method of molecular dynamics [30], which are today the most popular. Both predict that most sputtered atoms combine into diatomic clusters at a distance shorter than 6 Å from the surface. Remarkably, in accordance with the method of molecular dynamics, dimers form primarily from independently sputtered atoms, while the Monte Carlo method does not distinguish between direct emission and recombination: both mechanisms give equal contributions. This means that only those atoms may recombine that are the nearest neighbors on the emitting surface. That is, only strongly interacting atoms recombine. Since sputtered particles ionize at a distance shorter than 6 Å, the ionization of departing “pairs” of atoms can be considered as the ionization of a quasi-molecule. The ionization mechanism of resulting dimers will be the same as for sputtered atoms (see Eq. (1)). This brings up the reasonable question: why is the matrix

effect absent when some materials are analyzed using CsM cluster ions? In our earlier work [29], it was erroneously assumed that the ionization probability of all CsM clusters is close to unity. It was demonstrated in [31] with $CsAg^+$ that actually the ionization probability of CsM clusters is less than unity as a rule. Therefore, another explanation of the experimental data should be given.

To this end, we developed one more model of clustering during ion sputtering of the material. It was assumed that the overwhelming majority of CsM clusters result from direct emission [32]—emission of diatomic clusters as a whole. A minor amount of clusters that are produced by recombination of two independently sputtered particles can be considered as a partial case of direct emission. We may think so, because, as was mentioned above, this recombination takes place in the immediate vicinity of the surface, in which case the charge state of forming clusters and the independency of atom sputtering are out of the question. In other words, the recombination of some atoms is replaced by the emission of quasi-molecules, which appear on the surface in collision cascades initiated by a primary ion.

Mathematically, the emission of CsM^+ charged clusters is described by the relationship

$$I^+_{\mathrm{CsM}} = I_0 Y_{\mathrm{CsM}} \beta^+_{\mathrm{CsM}} \mathrm{Tr}_{\mathrm{CsM}}, \quad (3)$$

where Y_{CsM} is the probability of simultaneous emission of two atoms sputtered in the form of a molecule and β_{CsM} is the ionization probability of CsM clusters, which is given by a relationship similar to relationship (1) for the sputtered atom ionization,

$$\beta^+_{\mathrm{CsM}} \propto \exp\left[-\frac{I_p(\mathrm{CsM}) - \Phi^*}{\varepsilon_p}\right]. \quad (4)$$

Here, I_p(CsM) is the ionization potential of a CsM cluster and Φ^* is the work function of the target's surface exposed to cesium ions. Unfortunately, we could find only five cesium-containing dimers for which the ionization potential is known (Table 1). The lack of data for the ionization potentials of cesium-containing dimers seems to be the main reason why the direct emission model is disregarded by other researchers.

The work function of the ion-irradiated target also remains uncertain. It depends on a variety of factors, and the specifics of the respective dependences are under discussion. The experimental and theoretical values of the work function reported in the literature [5, 13, 15, 18, 19] are contradictory. With the aforesaid in mind, we began with gaining a deeper insight into the work function of a surface exposed to cesium ions.

WORK FUNCTION OF AN ION-IRRADIATED TARGET

Under experimental conditions similar to those used in this work, namely, target sputtering by 5.5-keV cesium ions incident at an angle of 42° to the surface normal, the work function decreases by 1.3 eV relative to the initial value [18]. Since the cesium ion beam energy in this work was 0.5 keV lower and the angle of incidence was 45°, we measured the work function of silicon and gallium arsenide targets, using the same technique as in [18], which consists in measuring a shift in the secondary ion energy distribution [18, 19] (see the previous section). We studied a shift in the energy distribution of secondary cesium ions as a function of the cesium ion irradiation dose up to the dose at which the shift of the energy spectra along the energy scale was no longer observed. Each measurement took about 25 s, and a total of 30 energy spectra were measured.

Table 1

M	Ionization potential CsM, eV		M	Ionization potential CsM, eV	
	calculation	experiment [42]		calculation	experiment [42]
Li	3.70	–	O	7.28	–
Na	3.68	4.05	Mg	3.84	–
K	3.46	–	Al	4.28	–
Cs	3.30	3.2	Si	5.24	–
F	8.4	8.8	Zn	3.86	–
Cl	7.76	7.84	Ga	4.07	–
I	6.72	7.9	As	5.61	–
C	5.93	–	Cd	3.82	–
N	6.26	–	–	–	–

The work function of the silicon and gallium arsenide surfaces versus the cesium ion irradiation dose (cesium ion fluence) is shown in Figs. 1a and 1b, respectively. Insets to both panels show the initial energy spectra. The zero shift of the work function was determined from its maximal value on the energy scale. It is seen that the maximal shift of the work function is $\Delta\Phi = 1.51$ and 0.58 eV for silicon and gallium arsenide, respectively. These values far exceed those obtained by Gnaser [18] presumably because of slightly differing sputtering conditions. Comparison between experimentally found shifts of the work function and those predicted by available models goes beyond this investigation.

Then, the experimental data were used to describe the sputtering of CsM^+ cluster ions. To this end, the work functions of the semiconductor targets exposed to cesium ions were estimated as the ionization potentials of these semiconductors with allowance for the band shift due to cesium ion implantation,

$$\Phi^*(\mathrm{Si}) = 4.05(A_{\mathrm{Si}}) + 1.1(E_g) - 1.51(\Delta\Phi) = 3.64 \text{ eV}$$

for the silicon surface and

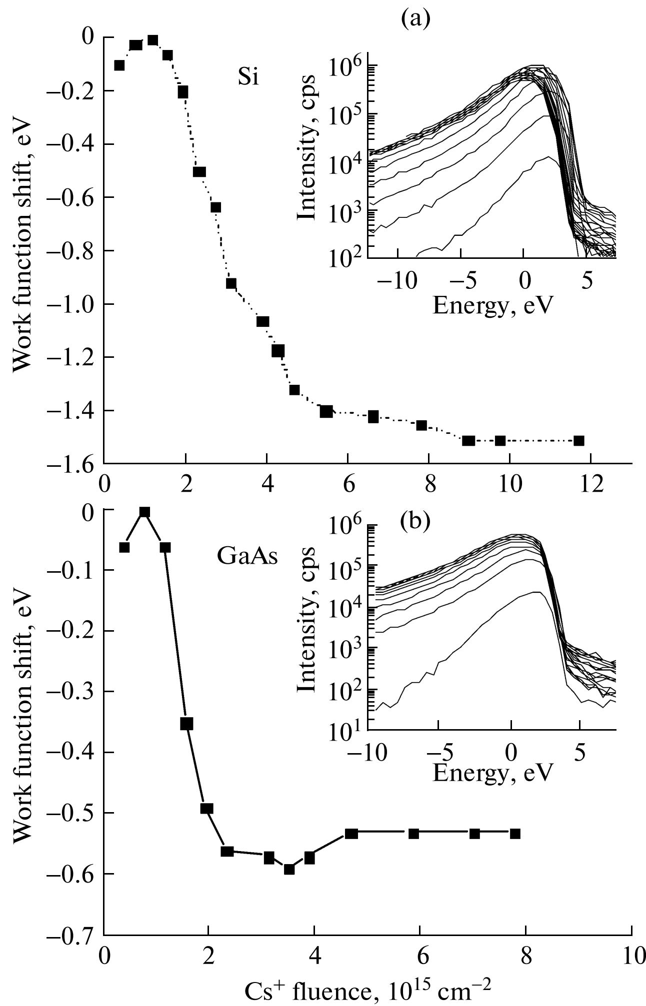

Fig. 1. Shift in the work function of the (a) Si and (b) GaAs surface vs. the cesium ion irradiation dose. The insets show the initial energy spectra.

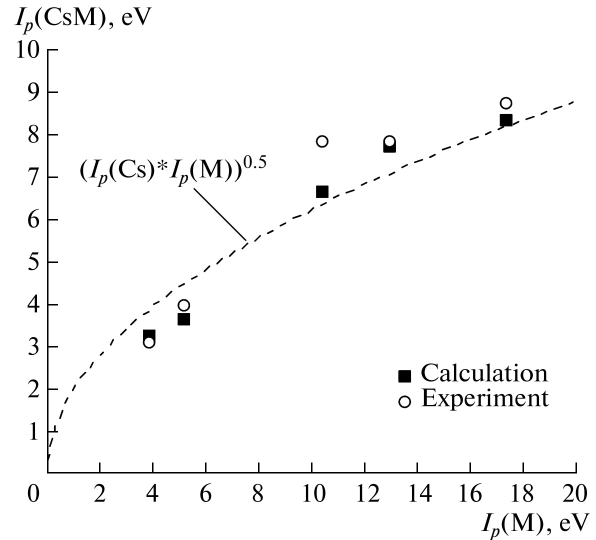

Fig. 2. Calculated ionization potentials for a number of CsM clusters vs. available experimental data. The ionization potentials are plotted against the ionization potentials of elements M.

$$\Phi^*(\text{GaAs}) = 4.07(A_{\text{GaAs}}) + 1.42(E_g) - 0.53(\Delta\Phi) = 4.96 \text{ eV}$$

for the gallium arsenide surface. Here, A_i is the electron affinity and E_g is the energy gap of the semiconductors [33] (see also Fig. 4). These values of the work function were used in formula (4) and compared with the ionization potentials of sputtered particles to estimate the secondary particle ionization probability.

However, prior to estimation of the CsM cluster ionization probability from formula (4), one should find the ionization potentials for CsM molecules.

IONIZATION POTENTIALS FOR CsM DIMERS

At the next stage of investigation, we calculated the ionization potentials of some CsM molecules that are of interest in relation to the problems being solved in this work. Calculations were carried out in terms of the density functional theory using the SIESTA computer program [34]. The most stable configuration of CsM molecules was determined by applying the conjugate gradient procedure with interaction forces, calculated in terms of the density functional theory in the generalized gradient approximation to the exchange correlation functional [35], and standard normally convergent relativistic potentials [36] in fully nonlocal form. These pseudopotentials were generated from the respective electron configuration (of valence electrons) in elements under consideration. We also considered a double-exponential polarized basis set with a threshold energy of 300 Ry to determine a spatial grid for numerical integration [37]. In simulation, free dimers relaxed until Hellmann–Feynman forces became lower than 1 meV/Å. In the adiabatic approximation, the theoretical ionization energy was found as the difference between the total energy of a neutral CsM molecule in the ground state and the energy of this molecule in the charged state (CsM^+), the latter being calculated for the same interatomic distances as in the neutral unexcited molecule.

Eventually, the theoretical ionization energy was calculated for alkali metals (Li, Na, K, Cs), halogens (F, Cl, I), and some other elements (C, N, O, Mg, Al, Si, Zn, Ga, As, Cd). The energy values are listed in Table 1, which also contains experimental data for the ionization potentials of some cesium-containing molecules.

These results allow us to draw some noteworthy conclusions and make a number of assumptions. First, the calculations are in good agreement with the experimental data, as follows from Fig. 2, which means that the calculations are correct. Then, it should be noted

that the ionization potentials of the cesium-containing dimers are considerably lower than those of their constituent atoms. Of special importance (in view of forthcoming considerations) is that the calculated ionization potentials of Cs_2 and CsK clusters are lower than the ionization potential of a Cs atom! This fact has interesting indirect support, and we will expand upon the point. A number of authors reported an inverse correlation between the ionization potential and polarizability of elements: namely, more readily polarizable elements have a lower ionization potential [38, 39]. Remarkably, such a correlation is observed not only for atoms but also for molecules [40, 41]. It is reasonable to suppose, in our opinion, that this correlation can also be expected for cesium-containing clusters. The polarizability of CsK and Cs_2 molecules equals 89 and 104 Å^3, respectively [42]. These values are much larger than the polarizability of a cesium atom (59.6 Å^3). Then, the ionization potentials calculated for Cs_2 and CsK appear quite acceptable.

According to Eqs. (1a) and (4), the ionization probability of a secondary particle exponentially depends on its ionization potential. We checked this dependence using earlier experimental data [29]. Figure 3 plots the relative sensitivity factor (RSF) against the calculated ionization potential of CsM^+ clusters, where M = C, O, N, Mg, Al, Ga, As, and Cd are elements implanted into GaN. Since the RSF of an element is defined as the flux of its secondary ions normalized to the ion current of a matrix element, it is inversely proportional to the ionization probability of the given secondary particle. The RSF data shown in Fig. 3 exponentially depend on the ionization potential of the dimers, which counts in favor of our model of CsM^+ cluster direct emission and indicates the validity of our ionization potential calculations for CsM molecules.

To prove conclusively that CsM clusters are the products of direct emission during target sputtering by a cesium beam, it is necessary to find a logical explanation for the weak matrix effect observed when CsM^+ clusters from a number of targets are analyzed. To do this, we will again turn to the calculated data for ionization potentials (Table 1). It is seen that while the ionization potentials of atoms vary from 3.89 (Cs) to 17.5 eV (F), those of the respective dimers vary in a much narrower interval from 3.3 (CsCs) to 8.47 eV (CsF). Additionally, the ionization potentials of clusters containing chemically similar elements, for example, alkali metals, are very close to each other. All this allows us to argue that, in the case of CsM clusters, the matrix effect is merely strongly reduced (compared with its amount in the case of atoms) because of a small spread in the ionization probabilities of these clusters, including when they are sputtered from different targets.

Thus, we determined the work function of the target exposed to cesium ions, calculated the ionization potentials of CsM clusters of interest, and confirmed the hypothesis of direct emission of these clusters. To design an experiment on measuring the cesium concentration on the sputtered surface, let us consider the band diagrams of silicon and gallium arsenide with allowance for the band bending induced by cesium ion implantation and determined from the change in the work function (Fig. 4). The main parameters of the semiconductors, namely, ionization potentials, bandgaps, and electron affinities [33], are indicated in Fig. 4, along with the ionization potentials of secondary Cs atoms and CsK, CsNa, Cs_2, CsSi, CsGa, and CsAs clusters. Comparing these ionization potentials with the ionization potential of the corresponding target (in this case, the ionization potential replaces the work function) allows us to uniquely interpret, based on the suggested ionization model (formula (4)), experimental data for emission of clusters from the Si and GaAs targets. Figure 5 shows the emission current of secondary Cs^+ ions and CsM^+ clusters (M is the matrix element of the above targets). The ionization probability reaches unity for secondary particles with an ionization potential lower than that of the target. For the gallium arsenide target, these are Cs atoms and CsK, CsNa, CsGa, and Cs_2 clusters. Note that the ionization probability of the CsAs cluster is smaller than unity (the exact value of this ionization probability is insignificant for our study). For the silicon target, only the ionization potentials of CsK and Cs_2 clusters are lower than that of the silicon; consequently, only for these clusters, one can expect 100% ionization. The remaining sputtered particles, namely, CsSi and CsNa clusters and Cs atoms have an ionization probability less than unity. In the experimental profiles depicted in Fig. 5, this shows up as nearly the same

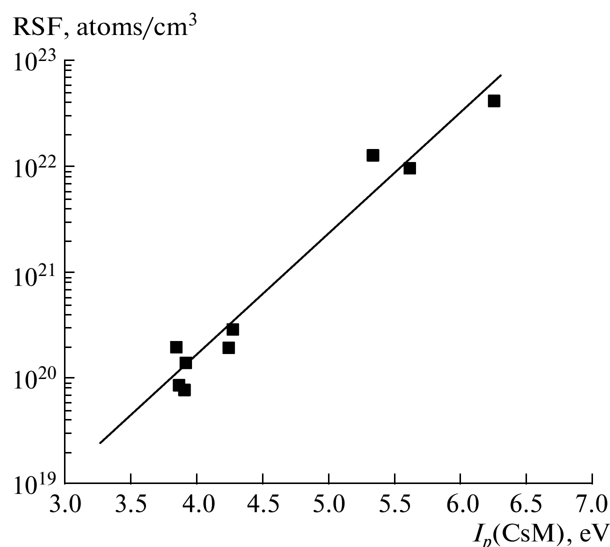

Fig. 3. RSF of CsM clusters sputtered by a cesium beam from a GaN target vs. the ionization potentials of these clusters (see data in Table 1).

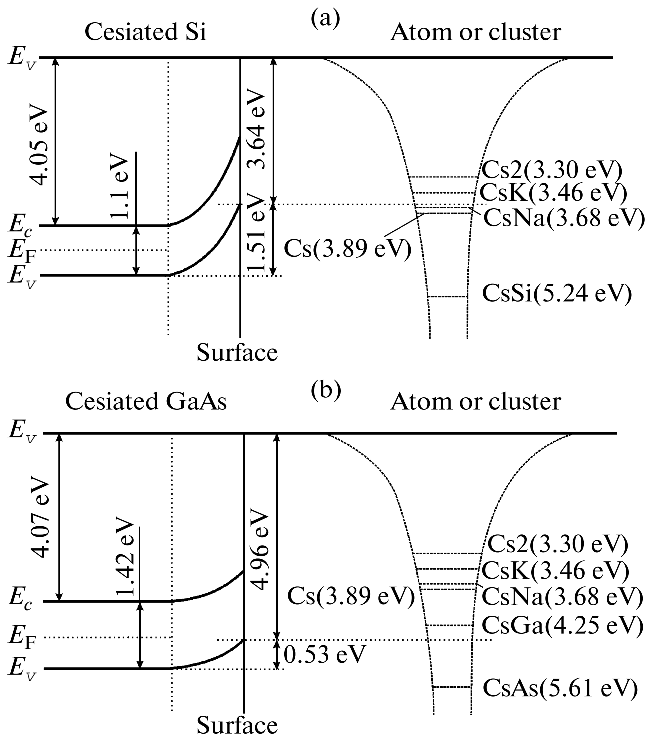

Fig. 4. Band diagrams of the (a) Si and (b) GaAs targets exposed to cesium ions. Shown are the electron affinities, ionization potentials, and bandgaps of the initial semiconductors and also the band bending (change in the work function) for the cesium-enriched surface. On the right, the ionization potentials of secondary particles (Cs and CsM clusters) are schematically shown.

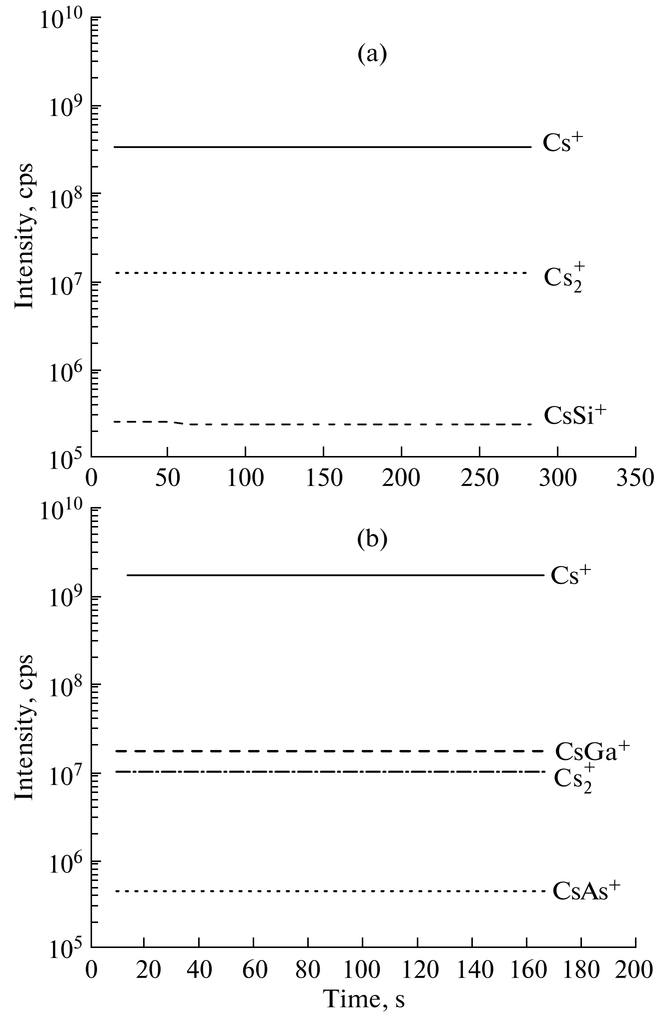

Fig. 5. Intensities of cesium secondary ions and some CsM^+ cluster ions sputtered from the (a) Si and (b) GaAs targets under steady-state sputtering conditions.

Cs_2^+ intensities for both targets (the ionization probability equals unity). At the same time, the Cs^+ intensity for the GaAs target is five times higher than for the Si target. In other words, if it is assumed that the ionization probability of secondary Cs atoms sputtered from GaAs is unity, that of secondary Cs atoms sputtered from Si is equal to 0.2.

As applied to the technique of determining the implanted cesium surface concentration, the most important fact following from the band diagrams and experimental profiles is that the ionization probability of sputtered CsK and Cs_2 clusters reaches unity for both targets; that is, we can put $\beta^+_{CsK} \equiv \beta^+_{Cs2} \approx 1$. Then, an experiment on determining the cesium surface concentration may be designed as follows: in the course of target irradiation by cesium ions and CsM^+ cluster ion detection, the layered distribution of implanted potassium ions is taken and the RSF of secondary CsK^+ clusters is measured.

Accurate to a coefficient depending on the difference between the emission probabilities of secondary Cs_2 and CsK clusters, Cs_2^+ clusters have the same RSF as CsK^+ clusters. In other words, the cesium concentration in the subsurface layer (which is implanted by cesium ions during sputtering) is qualitatively found by the procedure used to calculate the concentration from the ion current, as is done in standard SIMS analysis,

$$C_{Cs} = RSF(Cs_2^+)I(Cs_2^+)/I(CsM_m^+), \quad (5)$$

where I is the intensity of the cesium-containing cluster. In this work, the $RSF(Cs_2^+)$ is equated to the $RSF(CsK^+)$ for the silicon target. For the gallium arsenide target, the RSFs for CsK^+ and $CsNa^+$ were used (see below).

Figure 6 shows the experimental concentration distribution of the potassium implanted into the silicon target and also the distribution of cesium implanted into the target during ion sputtering and determined with the above technique.

The cesium concentration was found to be about 18 at %. This value was compared with those obtained by other methods under similar sputtering conditions (Table 2). Here, the data are seen to disagree. This problem was touched upon in the Introduction, where a large spread of published data, specifically, for the concentration of cesium implanted during ion sputtering, was noted. We guess that this spread arises because the sample is transferred from one high-vacuum system to another. Such a carryover causes hard-to-predict variations of the composition on the target's surface because of gas molecule adsorption. It was shown [8, 15] that even transferring in vacuum (under a residual pressure of 10^{-8} Torr) leads to the adsorption of a large amount of oxygen and carbon. One or more layers of adatoms introduce a considerable error into the cesium concentration determined on the etching surface. This is because, using conventional methods, say, Auger electron spectroscopy, one analyzes only a thin subsurface layer less than 1 nm thick [8]. Moreover, adsorbed oxygen (carbon) combines with the silicon to form a silicon oxide (silicon carbide) film, seemingly lowering the cesium concentration in the layer being analyzed (see, for example, data reported in [8]). After the ion beam is switched off, the surface reconfiguration and subsurface diffusion may take place because of oxygen and/or carbon deposition among other things.

In the case of X-ray photoelectron spectroscopy [7–10], an error in the cesium concentration may be caused by a large escape depth of photoelectrons, about 10 nm, which specifies the thickness of the analyzed layer. The thickness of the cesium-implanted layer is estimated as being smaller, about 5 nm. Accordingly, X-ray photoelectron spectroscopy also underestimates the cesium concentration. The method suggested in this work is free of the disadvantages listed above and provides a more correct value of the cesium concentration.

Earlier [43], a relationship was suggested for determining the surface concentration of ions implanted into a target being sputtered by these ions,

$$C_i \approx \frac{\delta}{Y_t k_p + \delta}. \quad (6)$$

Here, δ is the incorporation coefficient, which is usually taken to be equal to unity when target atoms are lighter than primary ions; Y_t is the target sputtering yield; and

$$k_p \approx (M_i/M_{Cs})^{2m}(U_t/U_{Cs})^{1-2m}$$

is the coefficient characterizing preferential sputtering of species (in this case, implanted cesium or target atoms) from the irradiated surface [44]. Table 2 lists cesium concentrations calculated by formula (6) with regard to experimentally found values of the sputtering yield: $Y = 3$ for silicon and $Y = 8.6$ for gallium arsenide. Shown also are the surface binding energy of elements calculated by the technique described in [45].

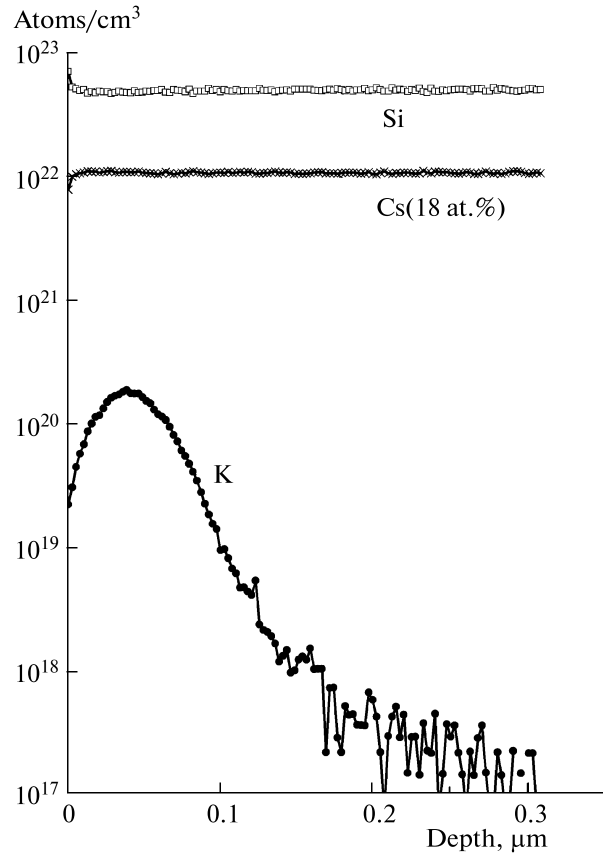

Fig. 6. Distribution profile of the potassium (monitored as CsK^+ cluster ions) implanted into the silicon in comparison with the concentration of the cesium (monitored as Cs_2^+ cluster ions) implanted during sputtering by the cesium ion beam (for details, see the text).

Good agreement between the calculated and experimental data support the assumptions made in this work.

When the same calculation was carried out for implanted sodium, the calculated cesium concentration turned out to be highly overestimated. As was

Table 2

	Cesium concentration, %	
	Si	GaAs
C^5_{Cs}, formula (6)	17.0	7.8
C^5_{Cs}, experiment	18.0	5.6–5.8
References	3.4 [10], 5.6 [12], 9 [11], 10 [8], 50 [17], 80 [9]	
Cesium surface binding energy U_{Cs}, eV	2.31	1.33
Target sputtering yield Y, atoms/ion	3.0	8.6

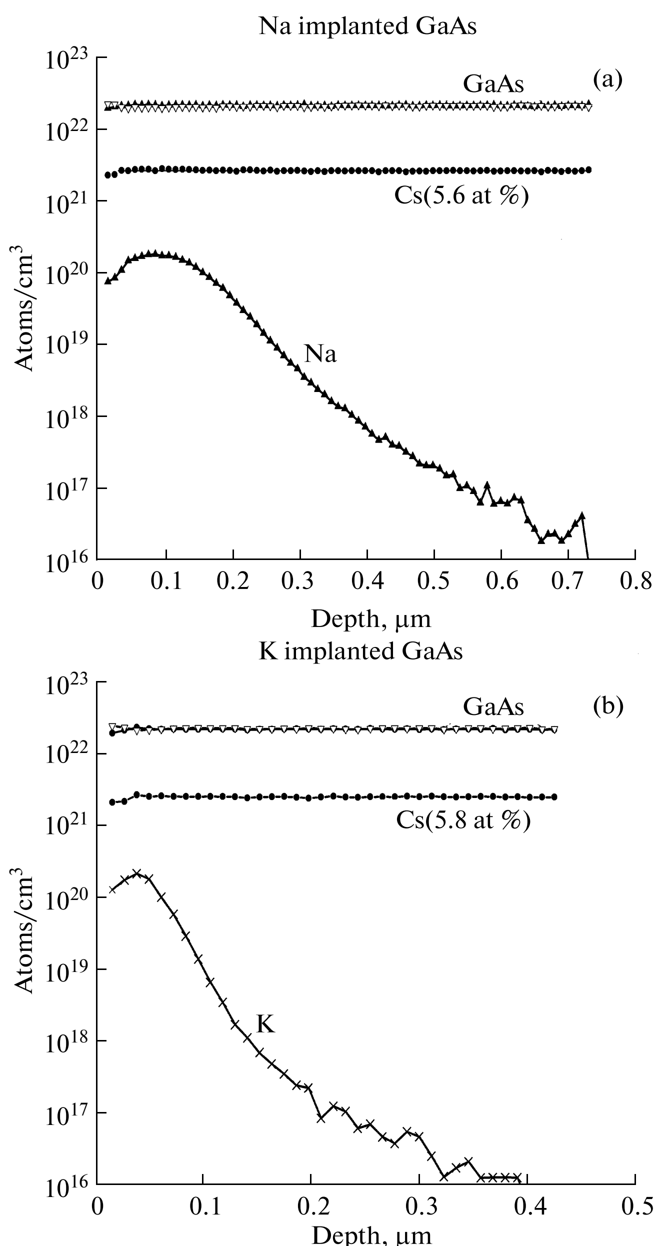

Fig. 7. Distribution profiles of (a) sodium and (b) potassium implanted into the GaAs target in comparison with the cesium concentration implanted during sputtering by the cesium ion beam and calculated by the suggested technique.

demonstrated earlier, the ionization probability of CsNa is less than unity (the ionization potential exceeds the work function of the surface, Fig. 4), so that this cluster cannot be used as an internal standard for calculation of the cesium concentration on silicon.

In the case of the GaAs target, we expected 100% ionization of both CsNa and CsK clusters with regard to the ionization potentials calculated for these clusters and the experimentally determined work function of the GaAs target (Fig. 4). Figure 7 shows the distributions of potassium and sodium implanted into the GaAs target, along with the calculated concentration of cesium implanted during sputtering. The experimental values of the cesium concentration obtained with CsK^+ and $CsNa^+$ used as internal standards are nearly the same: 5.8% and 5.6%, respectively. This discrepancy is attributed to the difference between the sputtering yield of these clusters and also between these clusters and the Cs_2 cluster. The discrepancy between the experimental and calculated concentrations can be regarded as insignificant, especially in comparison with the spread of experimental data reported by different authors [7–17].

CONCLUSIONS

It was shown that the formation of CsM^+ ions is best described by the model of direct emission of CsM clusters with their subsequent ionization by the same mechanism as the ionization of sputtered atoms. From ionization potentials calculated for some CsM molecules, conclusions are drawn that the ionization probability of sputtered CsK and Cs_2 molecules is close to unity. Then, using implanted potassium as an internal standard, one can determine the concentration of cesium ions implanted during sputtering. The cesium concentration thus determined on the Si and GaAs surfaces agree well with data calculated in terms of the adopted model.

Based on the ionization potentials and work functions of the Si and GaAs targets obtained in this work, a logical explanation for the absence of the matrix effect in III–V semiconductors can be suggested. From the band diagrams of Si and GaAs shown in Fig. 4, it follows that the ionization probability near unity can be expected for a number of molecules, such as CsGa, CsAl, CsMg, CsZn, CsCd (Table 1), and CsIn (the ionization potential was not calculated). The yield of these clusters from ternary and quaternary solid solutions of Group III and Group V elements (Al, Ga, In, P, As, Sb) does not depend on the solid solution composition (see, for example, [46]).

ACKNOWLEDGMENTS

This work was supported by the SENER-CONACYT Foundation, Mexico (grant. no. 152244, a group from CINVESTAV), and DGAPA-UNAM Foundation, Mexico (grant. no. IN102511, a group from UNAM).

REFERENCES

1. I. A. Abroyan, A. N. Andronov, and A. I. Titov, *Physical Foundations of Eelectron and Ion Technology* (Vysshaya Shkola, Moscow, 1984), p. 119.
2. A. Beninghoven, R. G. Rudenauer, and H. W. Werner, *Secondary Ion Mass Spectrometry: Basic Concepts, Instrumental Aspects, Application and Trends* (Wiley, New York, 1987), p. 310.

3. W. Reuter and K. Wittmaack, Appl. Surf. Sci. **5**, 221 (1980).
4. M. L. Yu, *Sputtering by Particle Bombardment III*, Ed. by R. Behrisch (Springer, Berlin, 1991), p. 91.
5. A. Villegas, Yu. Kudriavtsev, A. Godines, and R. Asomoza, Appl. Surf. Sci. **203–204**, 94 (2003).
6. Yu. Kudriavtsev and R. Asomoza, Nucl. Instrum. Methods Phys. Res. B **266**, 3540 (2008).
7. K. Wittmaack, P. Blank, and W. Wach, Radiat. Eff. **39**, 81 (1978).
8. N. Menzel and K. Wittmaack, Nucl. Instrum. Methods Phys. Res. B **191**, 235 (1981).
9. J. E. Chelgran, W. Katz, V. R. Deline, C. A. Evans, R. J. Blattner, and P. Williams, J. Vac. Sci. Technol. **16**, 324 (1979).
10. P. A. W. Van der Heide, Surf. Sci. **447**, 62 (2000).
11. A. Mikami, T. Okazawa, and Y. Kido, Jpn. J. Appl. Phys. **47**, 2234 (2008).
12. H. Tomizuka and A. Ayame, Appl. Surf. Sci. **89**, 281 (1995).
13. J. Brison and L. Houssiau, Nucl. Instrum. Methods Phys. Res. B **259**, 984 (2007).
14. J. Brison, R. G. Vitchev, and L. Houssiau, Nucl. Instrum. Methods Phys. Res. B **266**, 5159 (2008).
15. J. Brison, J. Guillot, B. Douhard, R. G. Vitchev, and L. Houssiau, Nucl. Instrum. Methods Phys. Res. B **267**, 519 (2009).
16. P. Chen, T. Janssens, and W. Vandervorst, Appl. Surf. Sci. **252**, 7239 (2006).
17. S. Yoshikawa, H. Morita, F. Toujou, T. Matsunaga, and K. Tsulamoto, Appl. Surf. Sci. **203–204**, 252 (2003).
18. H. Gnaser, Phys. Rev. B **54**, 16456 (1996).
19. H. Gnaser, Phys. Rev. B **54**, 17141 (1996).
20. Y. Gao, J. Appl. Phys. **64**, 3760 (1988).
21. H. Gnaser and H. Oechsner, Surf. Sci. Lett. **302**, L289 (1994).
22. C. W. Magee, W. L. Harrington, and E. M. Botnick, Int. J. Mass Spectrom. Ion Processes **103**, 45 (1990).
23. G. Prudon, B. Gautier, J. C. Dupuy, C. Dubois, M. Bonnear, J. Delmas, J. P. Vallard, G. Bremond, and R. Brenier, Thin Solid Films **294**, 54 (1997).
24. H. E. Smith, B.-H. Tsao, and J. Scofield, Mat. Sci. Forum. **527–529**, 629 (2006).
25. K. Wittmaack, *Proceedings of the 10th International Conference on Secondary Ion Mass Spectrometry, 1997*, Ed. by A. Benninghoven, B. Hagenhoff, and H. W. Werner (Wiley, Chichester, 1997), p. 39.
26. M. Gavelle, E. Schied, F. Cristiano, C. Armand, J.-M. Hartmann, Y. Campidelli, A. Halimaoui, P.-F. Fazzini, and O. Marcelot, J. Appl. Phys. **102**, 074904 (2007).
27. O. Koudriavtseva, A. Morales-Acevedo, Yu. Kudriavtsev, S. Gallardo, R. Asomoza, R. Mendoza-Perez, J. Sadtre-Hermandez, and G. Contreras-Puente, Appl. Surf. Sci. **255**, 1423 (2008).
28. W. Z. Gerhard, Z. Physik B **22**, 31 (1975).
29. Yu. Kudriavtsev, A. Villegax, A. Godines, and R. Asomoza, Appl. Surf. Sci. **206**, 187 (2003).
30. Y. Yamamura, *Proceedings of the 9th International Conference on Secondary Ion Mass Spectrometry, Yokohama, Japan, 1993*, Ed. by A. Benninghoven, et al. (Wiley, New York, 1994), p. 3.
31. S. Meyer, C. Staudt, and A. Wucher, Appl. Surf. Sci. **203–204**, 48 (2003).
32. V. I. Veksler, *Secondary Ion Emission in Metals* (Nauka, Moscow, 1978), p. 240.
33. http://www/ioffe.ru/index.php?row=14&subrow=0# (Site of Ioffe Physicotechnical Institute, Russian Academy of Sciences).
34. J. M. Soler, et al., J. Phys.: Condens. Matter. **14**, 2745 (2002).
35. J. P. Perdew, et al., Phys. Rev. Lett. **77**, 3865 (1996).
36. N. Troullier and J. L. Martins, Phys. Rev. B **43**, 1991 (1993).
37. L. Kleinman and D. M. Bylander, Phys. Rev. Lett. **48**, 1425 (1982).
38. I. K. Dmitrieva and G. I. Plindov, Phys. Scr. **27**, 402 (1983).
39. B. Fricke, J. Chem. Phys. **84**, 862 (1986).
40. T. M. Reed, J. Phys. Chem. **59**, 428 (1995).
41. K. R. S. Chandrakumar, T. K. Ghanty, and S. K. Ghosh, J. Phys. Chem. A **108**, 6661 (2004).
42. *Handbook of Chemistry and Physics*, Eds. by R. C. Weas and M. J. Astle (CRC, Boca Raton, 1983), pp. 1980–1981.
43. Yu. Kudriavtsev, Nucl. Instrum. Methods Phys. Res. B **160**, 307 (2000).
44. P. Sigmund, *Sputtering by Ion Bombardment: Theoretical Concepts. Sputtering by Particle Bombardment I*, Ed. by R. Behrisch (Springer, Berlin, 1981), p. 18.
45. Y. Kudriavtsev, A. Villegas, A. Godines, and R. Asomoza, Appl. Surf. Sci. **239**, 273 (2005).
46. A. P. Kovarsky, Yu. L. Kretser, Yu. A. Kudriavtsev, D. N. Stroganov, M. A. Yagovkina, T. Beierlein, and S. Strike, MRS Internet J. Nitride Semicond. Res. **3**, 10 (1998).

Translated by V. Isaakyan